Stereoselective Formation of Mono- and Di-Hydroxylated Polychlorinated Biphenyls by Rat Cytochrome P450 2B1

Zhe Lu[1, §], Izabela Kania-Korwel[2, §], Hans-Joachim Lehmler[2, *], and Charles S. Wong[1, 3, *]

[1]Department of Chemistry, University of Manitoba, Winnipeg, MB, R3T 2N2, Canada;

[2]Department of Occupational and Environmental Health, College of Public Health, University of Iowa, Iowa City, Iowa 52242,United States;

[3]Department of Environmental Studies and Sciences and Department of Chemistry, Richardson College for the Environment, University of Winnipeg, Winnipeg, MB, R3B 2E9, Canada.

[§] Two authors have same contributions to this manuscript.

*Corresponding authors:

Lehmler--Phone: +1-319-335-4310; Fax: +1-319-335-4290; E-mail: hans-joachim-lehmler@uiowa.edu

Wong--Phone: +1-204-786-9335; Fax: +1-204-775-2114; E-mail: wong.charles.shiu@alum.mit.edu

EXPERIMENTAL SECTION

Experiment design for the section "Interference between the two atropisomers of PCB 136" in the manuscript

Initial substrate amounts for experiments to study interference between the two atropisomers of PCB 136:

Incubation 1: 500 ng (-)-PCB 136+0 ng (+)-PCB 136;

Incubation 2: 500 ng (-)-PCB 136+100 ng (+)-PCB 136;

Incubation 3: 500 ng (-)-PCB 136+250 ng (+)-PCB 136;

Incubation 4: 500 ng (-)-PCB 136+500 ng (+)-PCB 136;

Incubation 5: 0 ng (-)-PCB 136+500 ng (+)-PCB 136;

Incubation 6: 100 ng (-)-PCB 136+500 ng (+)-PCB 136;

Incubation 7: 250 ng (-)-PCB 136+500 ng (+)-PCB 136.

Incubation 8: 500 ng (-)-PCB 136+500 ng (+)-PCB 136+CYP control---negative control

The incubations were repeated in triplicate for each condition.

Results

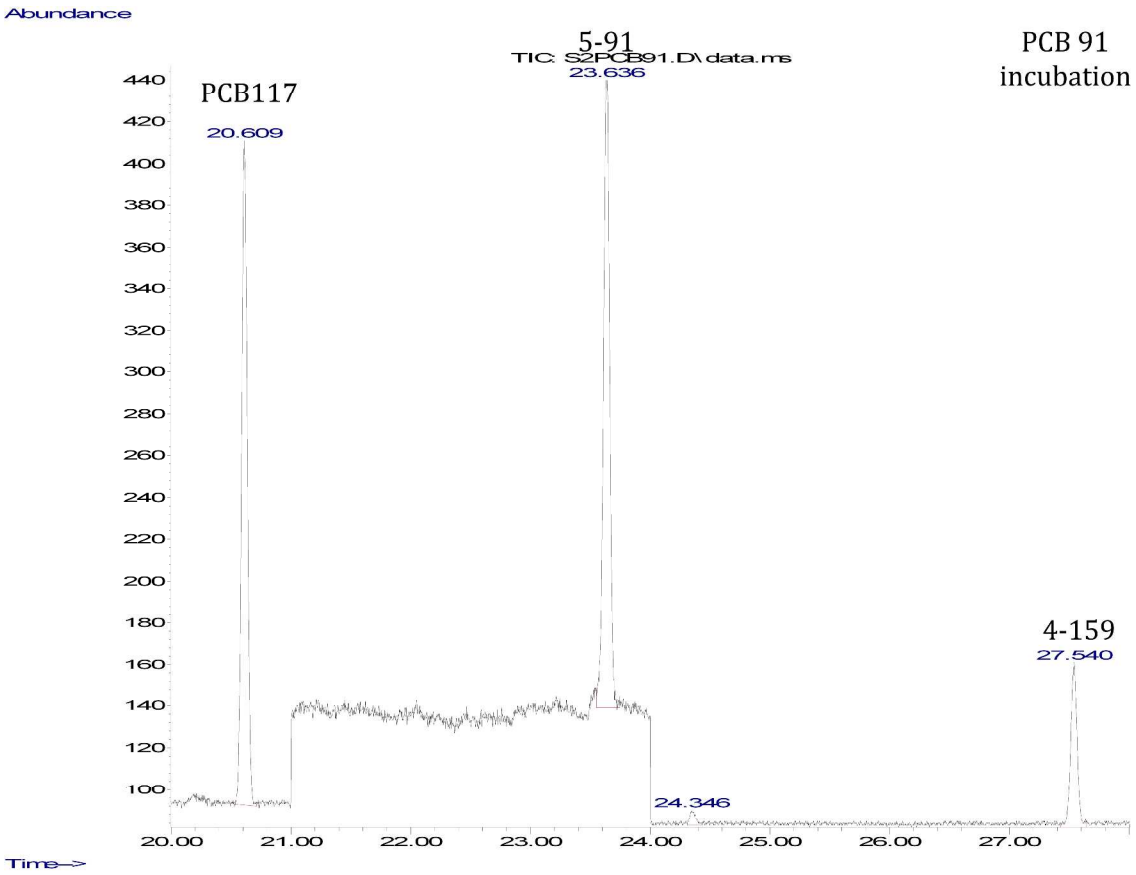

Figure S1A: Metabolites of PCB 91 formed by rat CYP2B1. GC-MS chromatogram of a PCB 91 incubation sample recorded in SIM mode.

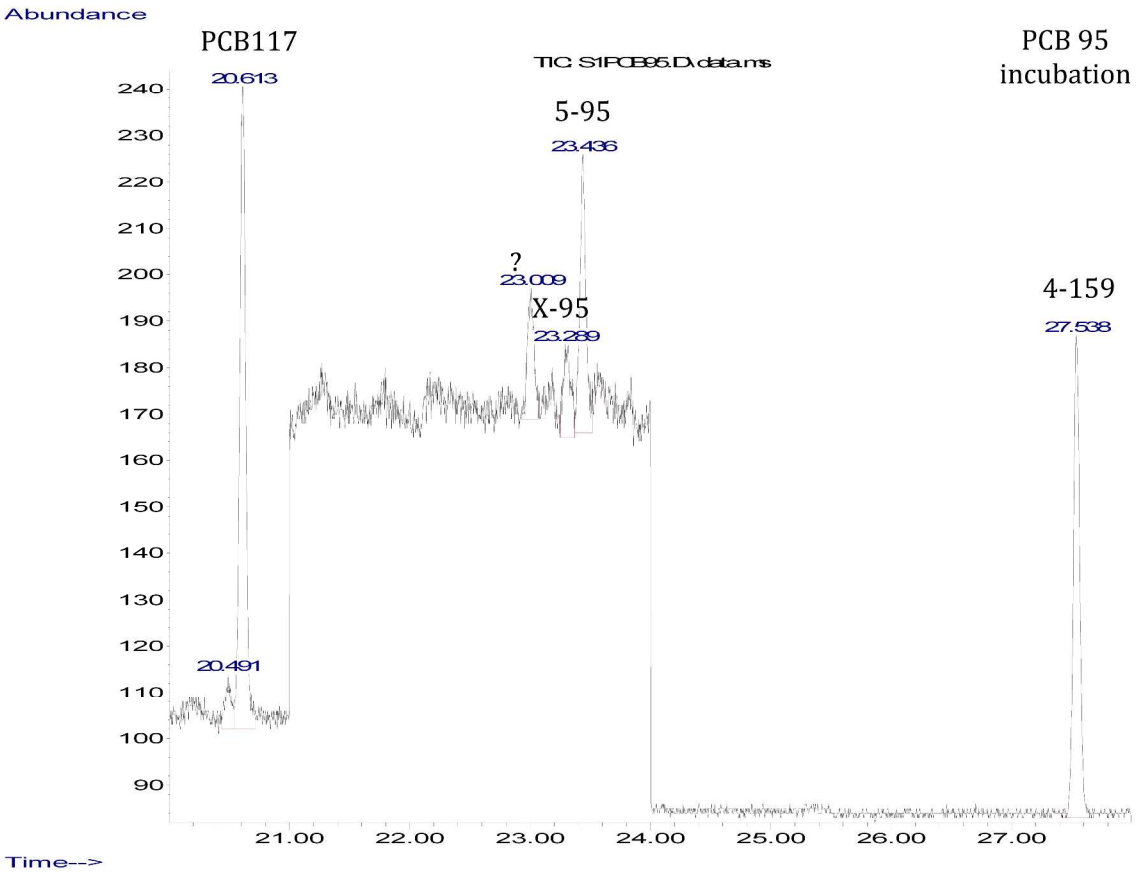

Figure S1B: Metabolites of PCB 95 formed by rat CYP2B1. GC-MS chromatogram of a PCB 95 incubation sample recorded in SIM mode. Peaks at 23.009 and 23.289 min are currently unidentified mono-hydroxylated metabolites of PCB 95. The peak at 23.289 min (X-95) was previously observed in incubations with rat liver microsomes.[1]

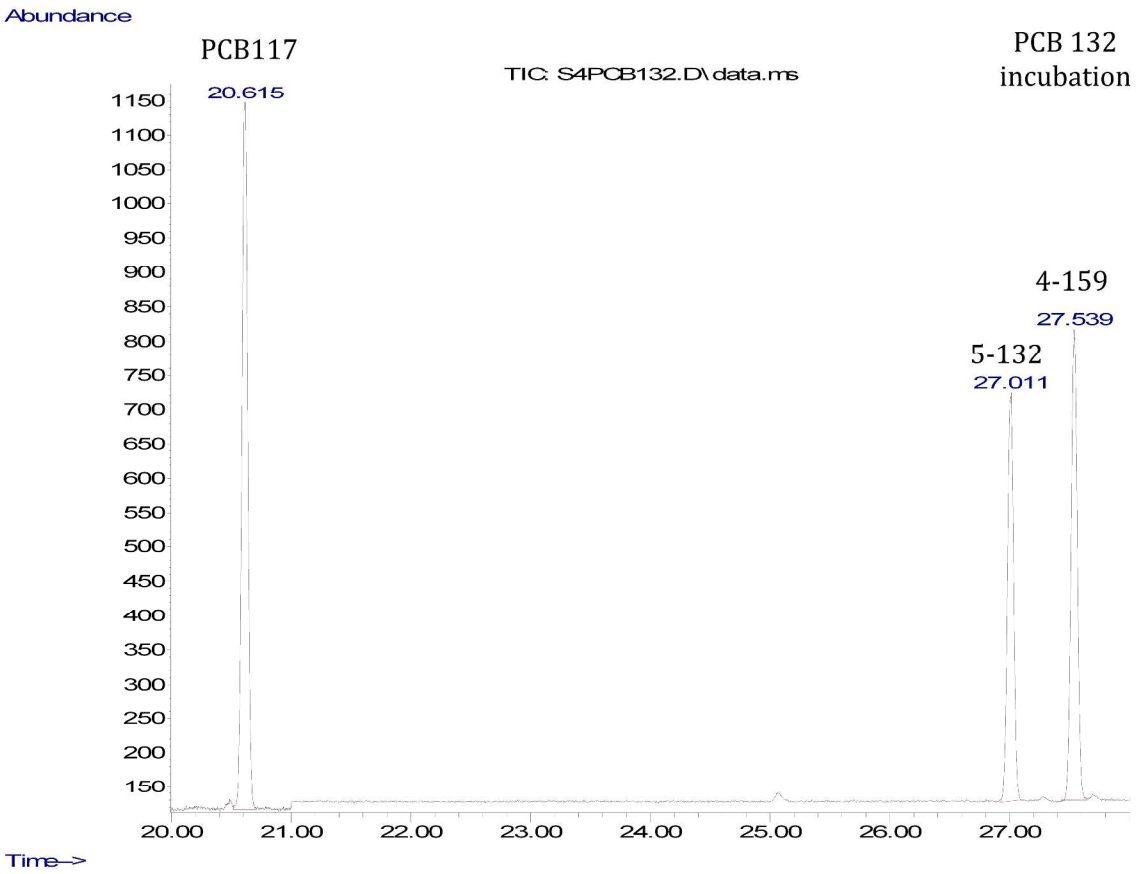

Figure S1C: Metabolites of PCB 132 formed by rat CYP2B1. GC-MS chromatogram of a PCB 132 incubation sample recorded in SIM mode.

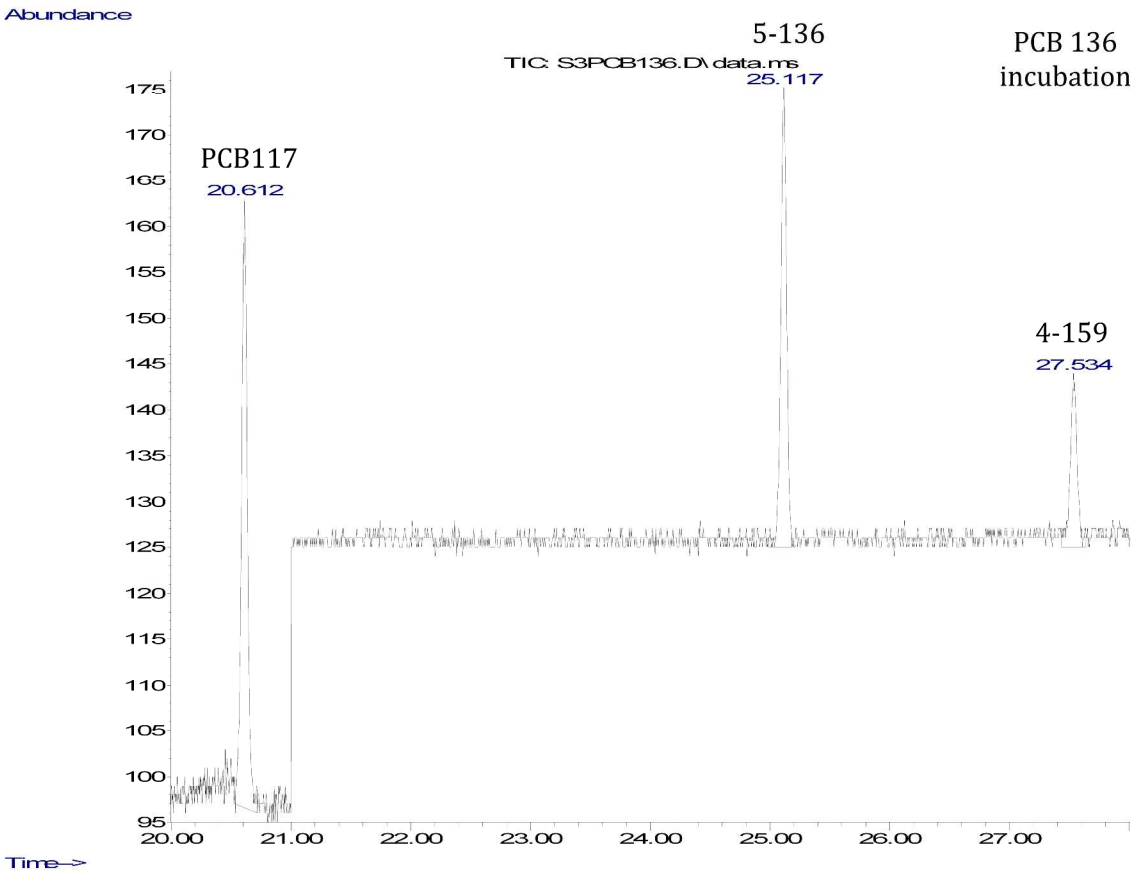

Figure S1D: Metabolites of PCB 136 formed by rat CYP2B1. GC-MS chromatogram of a PCB 136 incubation sample were recorded in SIM mode.

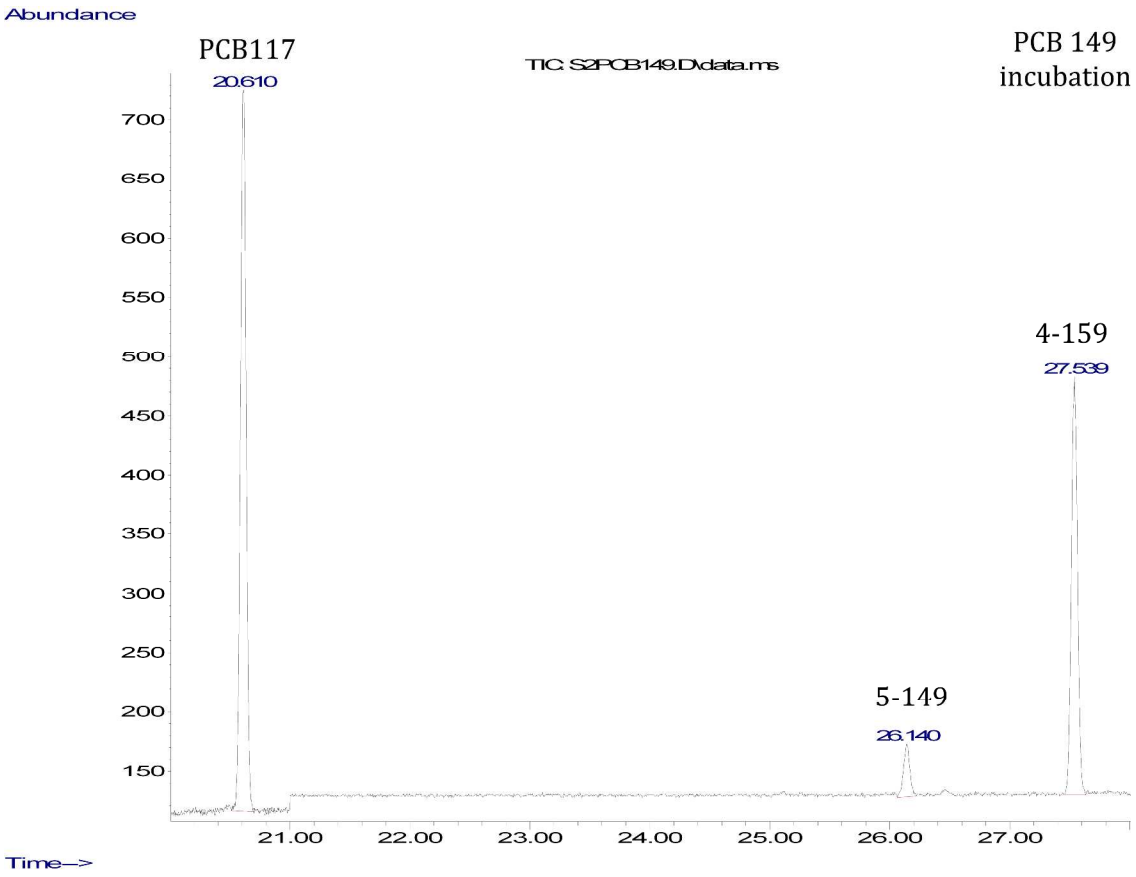

Figure S1E: Metabolites of PCB 149 formed by rat CYP2B1. GC-MS chromatogram of a PCB 149 incubation sample recorded in SIM mode.

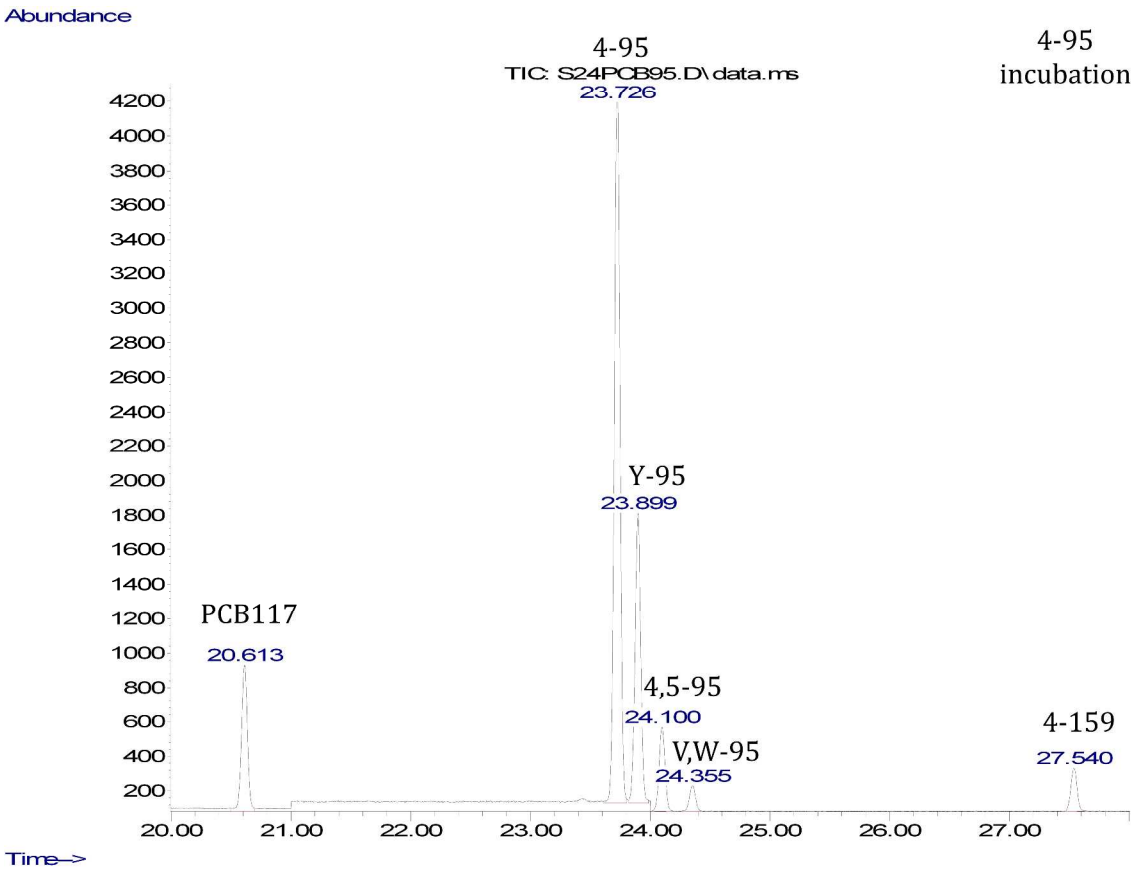

Figure S2A: Metabolites of 4-95 formed by rat CYP2B1. GC-MS chromatogram of a 4-95 incubation sample recorded in SIM mode. The peak at 23.899 min (Y-95) is a currently unidentified mono-hydroxylated metabolite. The peak at 24.355 min (V,W-95) is a unknown dihydroxylated metabolite.

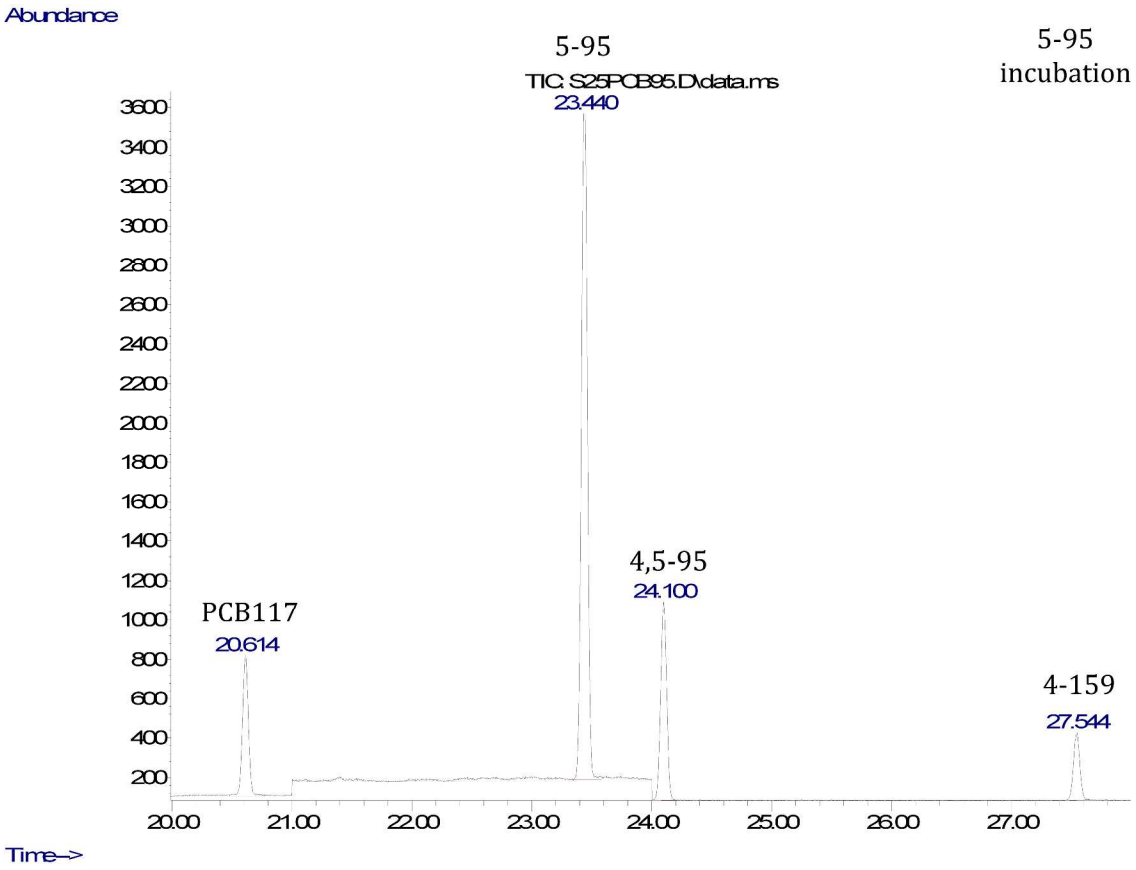

Figure S2B: Metabolites of 5-95 formed by rat CYP2B1. GC-MS chromatogram of a 5-PCB 95 incubation sample recorded in SIM mode.

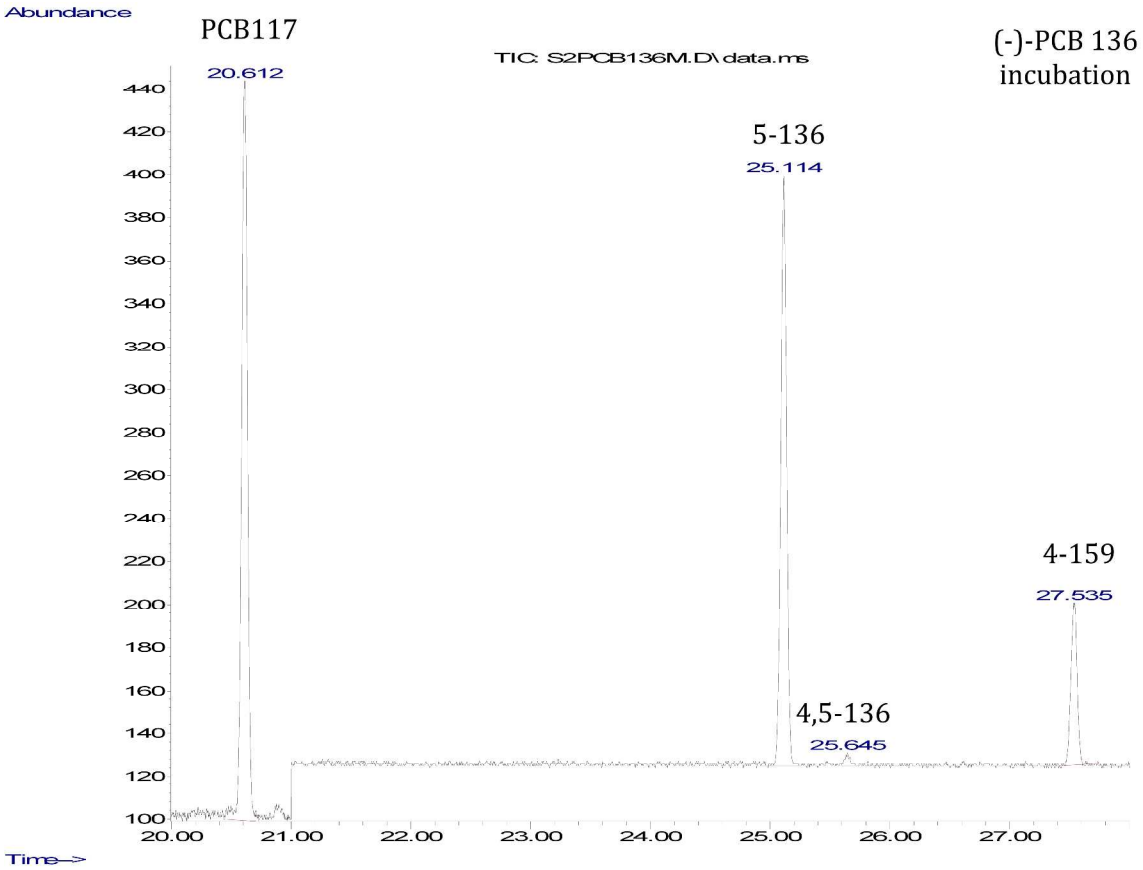

Figure S3A: Metabolites of (-)-PCB 136 formed by rat CYP2B1. GC-MS chromatogram of a (-)-PCB 136 incubation sample recorded in SIM mode.

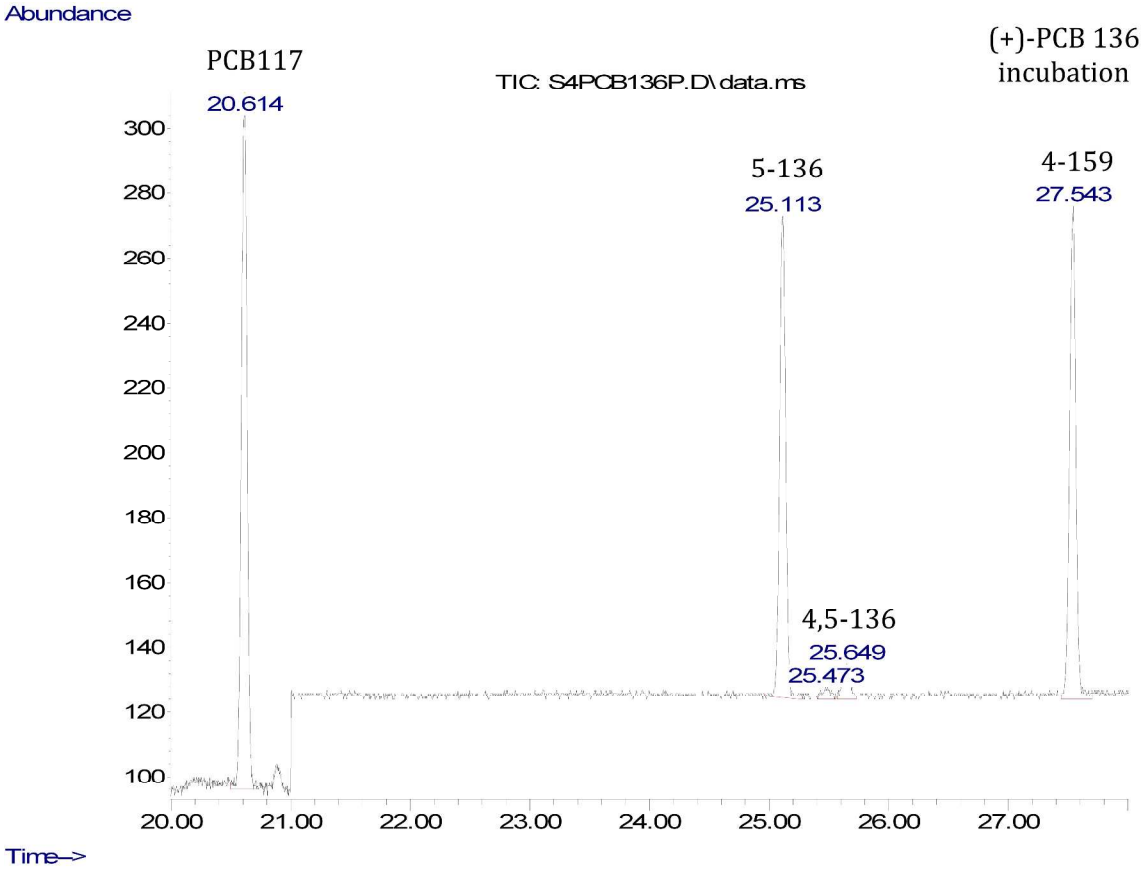

Figure S3B: Metabolites of (+)-PCB 136 formed by rat CYP2B1. GC-MS chromatogram of a (+)-PCB 136 incubation sample recorded in SIM mode.

Table S1 Comparison of Enantiomer Fractions (EFs) of 5-OH-PCB metabolites from different studies.

5-OH-PCBs	Present study Rat CYP2B1	Rat liver microsomes [1,2]	Rat liver slices [3]	Rat *in vivo* [4]	Mice *in vivo* [5]
5-91	0.17	0.54			
5-95	0.20	0.36			0.65
5'-132	0.85	0.30			
5-136	0.77	0.70	0.69~0.74	0.40	
5-149	0.41	0.66			

Table S2 Raw data of biotransformation activities of chiral PCBs and formation activities of mono- and di-OH-PCBs (Please see Fig.1 in the manuscript for summary). N.D.= not detected. The initial concentration of each atropisomer of chiral PCBs was 500 ng/mL.

PCBs	Biotransformation activities of E1 (ng PCB/mL/pmol CYP2B1/min)			Biotransformation activities of E2 (ng PCB/mL/pmol CYP2B1/min)		
	Sample 1	Sample 2	Sample 3	Sample 1	Sample 2	Sample 3
PCB 91	3.57×10^{-1}	2.12×10^{-1}	2.30×10^{-1}	1.85×10^{-1}	1.18×10^{-1}	1.29×10^{-1}
PCB 95	3.67×10^{-2}	8.67×10^{-2}	5.67×10^{-2}	2.07×10^{-1}	2.20×10^{-1}	2.33×10^{-1}
PCB 132	1.49×10^{-1}	1.42×10^{-1}	1.65×10^{-1}	4.71×10^{-2}	9.82×10^{-3}	4.13×10^{-2}
PCB 136	1.58×10^{-1}	1.43×10^{-1}	1.22×10^{-1}	2.30×10^{-1}	2.17×10^{-1}	1.88×10^{-1}
PCB 149	3.50×10^{-2}	2.33×10^{-2}	2.17×10^{-2}	4.05×10^{-2}	2.70×10^{-2}	2.70×10^{-2}

Parent PCBs	*para*-OH-PCBs (ng OH-PCB/mL/pmol CYP2B1/min)			*meta*-OH-PCBs (ng OH-PCB/mL/pmol CYP2B1/min)			*para,meta*-diOH-PCBs (ng diOH-PCB/mL/pmol CYP2B1/min)		
	Sample1	Sample2	Sample 3	Sample1	Sample 2	Sample 3	Sample1	Sample2	Sample 3
PCB 91	8.17×10^{-4}	N.D.	8.50×10^{-4}	8.17×10^{-2}	6.79×10^{-2}	1.20×10^{-1}	1.70×10^{-3}	2.65×10^{-3}	5.95×10^{-3}
PCB 95	N.D.	N.D.	N.D.	2.66×10^{-1}	1.22×10^{-1}	2.58×10^{-1}	N.D.	N.D.	N.D.
PCB 132	N.D.	N.D.	N.D.	7.31×10^{-2}	1.46×10^{-1}	7.66×10^{-2}	N.D.	N.D.	N.D.
PCB 136	2.78×10^{-3}	N.D.	1.32×10^{-3}	3.77×10^{-1}	3.16×10^{-1}	3.03×10^{-1}	1.00×10^{-2}	4.97×10^{-3}	7.17×10^{-3}
PCB 149	N.D.	N.D.	N.D.	3.12×10^{-2}	2.70×10^{-2}	2.44×10^{-2}	N.D.	N.D.	N.D.

Table S3 Raw data of biotransformation activities of OH-PCB 95 and formation activities of 4,5-diOH-PCBs (Please see Fig.2 in the manuscript for summary). The initial concentration of each atropisomer of 4-95 or 5-95 was 500 ng/mL.

Substrate (OH-PCB 95)	Biotransformation activities of OH-PCB 95 (ng OH-PCB/mL/pmol CYP2B1/min)			Formation activities of 4,5-diOH-PCBs (ng diOH-PCB/mL/pmol CYP2B1/min)		
	Sample 1	Sample 2	Sample 3	Sample 1	Sample 2	Sample 3
4-95	5.77×10^{-1}	5.78×10^{-1}	8.48×10^{-1}	2.65×10^{-1}	2.76×10^{-1}	3.08×10^{-1}
5-95	8.35×10^{-1}	9.78×10^{-1}	8.60×10^{-1}	4.30×10^{-1}	4.50×10^{-1}	5.50×10^{-1}

Table S4 Raw data of biotransformation and product formation activities interference between two atropisomers of PCB 136 (Please see Fig.3 and 4 in the manuscript for summary)

Biotransformation activities of (-)-PCB 136 (ng (-)-PCB 136/mL/pmol CYP2B1/min)				
	500 ng/mL (-)-PCB 136 + different initial concentration of (+)-PCB 136 (ng/mL) as competitor			
	0 ng/mL	100 ng/mL	250 ng/mL	500 ng/mL
Sample 1	4.41×10^{-1}	2.21×10^{-1}	9.45×10^{-2}	1.53×10^{-1}
Sample 2	4.41×10^{-1}	2.48×10^{-1}	1.44×10^{-1}	1.08×10^{-1}
Sample 3	3.33×10^{-1}	2.30×10^{-1}	8.55×10^{-2}	1.26×10^{-1}
Biotransformation activities of (+)-PCB 136 (ng (+)-PCB 136/mL/pmol CYP2B1/min)				
	500 ng/mL (-)-PCB 136 + different initial concentration of (+)-PCB 136 (ng/mL) as competitor			
	0 ng/mL	100 ng/mL	250 ng/mL	500 ng/mL
Sample 1	0	3.15×10^{-2}	1.80×10^{-1}	2.70×10^{-1}
Sample 2	0	9.90×10^{-2}	2.43×10^{-1}	4.19×10^{-1}
Sample 3	0	9.00×10^{-2}	1.80×10^{-1}	3.11×10^{-1}
Formation activities of 5-OH-PCB 136 (ng OH-PCB/mL/pmol CYP2B1/min)				
	500 ng/mL (-)-PCB 136 + different initial concentration of (+)-PCB 136 (ng/mL) as competitor			
	0 ng/mL	100 ng/mL	250 ng/mL	500 ng/mL
Sample 1	2.28×10^{-1}	2.66×10^{-1}	2.72×10^{-1}	2.96×10^{-1}
Sample 2	2.50×10^{-1}	2.78×10^{-1}	2.40×10^{-1}	2.71×10^{-1}
Sample 3	2.42×10^{-1}	2.86×10^{-1}	3.13×10^{-1}	3.13×10^{-1}
Formation activities of 4-OH-PCB 136 (ng OH-PCB/mL/pmol CYP2B1/min)				
	500 ng/mL (-)-PCB 136 +different initial concentration of (+)-PCB 136 (ng/mL) as competitor			
	0 ng/mL	100 ng/mL	250 ng/mL	500 ng/mL
Sample 1	2.78×10^{-3}	1.78×10^{-3}	2.00×10^{-3}	1.22×10^{-3}
Sample 2	3.89×10^{-3}	1.78×10^{-3}	1.11×10^{-3}	1.11×10^{-3}
Sample 3	4.11×10^{-3}	3.33×10^{-3}	2.67×10^{-3}	1.33×10^{-3}
Formation activities of 4,5-diOH-PCB 136 (ng diOH-PCB/mL/pmol CYP2B1/min)				
	500 ng/mL (-)-PCB 136 + different initial concentration of (+)-PCB 136 (ng/mL) as competitor			
	0 ng/mL	100 ng/mL	250 ng/mL	500 ng/mL
Sample 1	1.60×10^{-2}	9.89×10^{-3}	1.89×10^{-3}	5.67×10^{-3}
Sample 2	3.00×10^{-2}	2.24×10^{-2}	9.44×10^{-3}	9.33×10^{-3}
Sample 3	1.50×10^{-2}	3.33×10^{-3}	7.78×10^{-3}	3.00×10^{-3}

Biotransformation activities of (+)-PCB 136 (ng (+)-PCB 136/mL/pmol CYP2B1/min)				
	500 ng/mL (+)-PCB 136 + different initial concentration of (-)-PCB 136 (ng/mL) as competitor			
	0 ng/mL	100 ng/mL	250 ng/mL	500 ng/mL
Sample 1	3.83×10^{-1}	2.30×10^{-1}	2.48×10^{-1}	2.70×10^{-1}
Sample 2	3.15×10^{-1}	2.79×10^{-1}	2.79×10^{-1}	4.19×10^{-1}
Sample 3	3.12×10^{-1}	2.39×10^{-1}	2.52×10^{-1}	3.11×10^{-1}
Biotransformation activities of (-)-PCB 136 (ng (-)-PCB 136/mL/pmol CYP2B1/min)				
	500 ng/mL (+)-PCB 136 + different initial concentration of (-)-PCB 136 (ng/mL) as competitor			
	0 ng/mL	100 ng/mL	250 ng/mL	500 ng/mL
Sample 1	0	3.15×10^{-2}	1.08×10^{-1}	1.53×10^{-1}
Sample 2	0	3.60×10^{-2}	9.90×10^{-2}	1.08×10^{-1}
Sample 3	0	6.75×10^{-2}	9.00×10^{-2}	1.26×10^{-1}
Formation activities of 5-OH-PCB 136 (ng OH-PCB/mL/pmol CYP2B1/min)				
	500 ng/mL (+)-PCB 136 + different initial concentration of (-)-PCB 136 (ng/mL) as competitor			
	0 ng/mL	100 ng/mL	250 ng/mL	500 ng/mL
Sample 1	2.89×10^{-1}	3.38×10^{-1}	3.07×10^{-1}	2.96×10^{-1}
Sample 2	2.93×10^{-1}	2.92×10^{-1}	2.87×10^{-1}	2.71×10^{-1}
Sample 3	3.04×10^{-1}	3.04×10^{-1}	2.94×10^{-1}	3.13×10^{-1}
Formation activities of 4-OH-PCB 136 (ng OH-PCB/mL/pmol CYP2B1/min)				
	500 ng/mL (+)-PCB 136 +different initial concentration of (-)-PCB 136 (ng/mL) as competitor			
	0 ng/mL	100 ng/mL	250 ng/mL	500 ng/mL
Sample 1	8.89×10^{-4}	7.78×10^{-4}	1.33×10^{-3}	1.22×10^{-3}
Sample 2	6.67×10^{-4}	4.44×10^{-4}	1.00×10^{-3}	1.11×10^{-3}
Sample 3	6.67×10^{-4}	7.78×10^{-4}	1.44×10^{-3}	1.33×10^{-3}
Formation activities of 4,5-diOH-PCB 136 (ng diOH-PCB/mL/pmol CYP2B1/min)				
	500 ng/mL (+)-PCB 136 + different initial concentration of (-)-PCB 136 (ng/mL) as competitor			
	0 ng/mL	100 ng/mL	250 ng/mL	500 ng/mL
Sample 1	6.78×10^{-3}	7.56×10^{-3}	6.89×10^{-3}	5.67×10^{-3}
Sample 2	9.33×10^{-3}	9.22×10^{-3}	9.11×10^{-3}	9.33×10^{-3}
Sample 3	4.67×10^{-3}	6.33×10^{-3}	7.11×10^{-3}	3.00×10^{-3}

References

1. Kania-Korwel, I.; Duffel, M. W.; Lehmler, H.-J. Gas chromatographic analysis with chiral cyclodextrin phases reveals the enantioselective formation of hydroxylated polychlorinated biphenyls by rat liver microsomes. *Environ. Sci. Technol.* **2011**, *45*, 9590-9596.

2. Wu, X.; Pramanik, A.; Duffel, M. W.; Hrycay, E. G.; Bandiera, S. M.; Lehmler, H.-J.; Kania-Korwel, I. 2, 2′, 3, 3′, 6, 6′-Hexachlorobiphenyl (PCB 136) is enantioselectively oxidized to hydroxylated metabolites by rat liver microsomes. *Chem. Res. Toxicol.* **2011**, *24*, 2249-2257.

3. Wu, X.; Kania-Korwel, I.; Chen, H.; Stamou, M.; Dammanahalli, K.J.; Duffel, M.; Lein, P.J.; Lehmler, H.-J. Metabolism of 2,2',3,3',6,6'-hexachlorobiphenyl (PCB 136) atropisomers in tissue slices from phenobarbital or dexamethasone-induced rats is sex-dependent. *Xenobiotica* **2013**; DOI 10.3109/00498254.2013.785626.

4. Kania-Korwel, I.; Vyas, S. M.; Song, Y.; Lehmler, H.-J. Gas chromatographic separation of methoxylated polychlorinated biphenyl atropisomers. *J. Chromatogr. A* **2008**, *1207*, 146-154.

5. Kania-Korwel, I.; Barnhart, C. D.; Stamou, M.; Truong, K. M.; El-Komy, M. H.; Lein, P. J.; Veng-Pedersen, P.; Lehmler, H.-J. 2,2′,3,5′,6-pentachlorobiphenyl (PCB 95) and its hydroxylated metabolites are enantiomerically enriched in female mice. *Environ. Sci. Technol.* **2012**, *46*, 11393-11401.